Research

New Phytologist

The evolution of ectomycorrhizal symbiosis in the Late Cretaceous is a key driver of explosive diversification in Agaricomycetes

Hirotoshi Sato

Graduate School of Human and Environmental Studies, Kyoto University, Sakyo, Kyoto 606-8501, Japan

Author for correspondence:
Hirotoshi Sato
Email: h-sato@sys.bot.kyoto-u.ac.jp

Received: *29 March 2023*
Accepted: *15 May 2023*

New Phytologist (2024) **241:** 444–460
doi: 10.1111/nph.19055

Key words: adaptive radiation, Basidiomycota, coevolutionary diversification, ecological opportunity, evolutionary diversification, evolutionary priority effect, explosive diversification, mutualistic symbiosis.

Summary

- Ectomycorrhizal (EcM) symbiosis, a ubiquitous plant–fungus interaction in forests, evolved in parallel in fungi. Why the evolution of EcM fungi did not necessarily increase ecological opportunities for explosive diversification remains unclear. This study aimed to reveal the driving mechanism of the evolutionary diversification in the fungal class Agaricomycetes, specifically by testing whether the evolution of EcM symbiosis in the Late Cretaceous increased ecological opportunities.
- The historical character transitions of trophic state and fruitbody form were estimated based on phylogenies inferred from fragments of 89 single-copy genes. Moreover, five analyses were used to estimate the net diversification rates (speciation rate minus extinction rate).
- The results indicate that the unidirectional evolution of EcM symbiosis occurred 27 times, ranging in date from the Early Triassic to the Early Paleogene. The increased diversification rates appeared to occur intensively at the stem of EcM fungal clades diverging in the Late Cretaceous, coinciding with the rapid diversification of EcM angiosperms. By contrast, the evolution of fruitbody form was not strongly linked with the increased diversification rates.
- These findings suggest that the evolution of EcM symbiosis in the Late Cretaceous, supposedly with coevolving EcM angiosperms, was the key drive of the explosive diversification in Agaricomycetes.

Introduction

An understanding of what triggers explosive diversification has been a central topic in evolutionary biology since Darwin. A burst of diversification occurs when speciation is facilitated by new ecological opportunities, particular environments, and ecological niches not filled by competing taxa (Simpson, 1953; Schluter, 2000; Losos, 2010). Ecological opportunities become available in a number of ways, such as through the evolution of key morphological or functional traits, dispersal into a new habitat, and mass extinction of competing lineages (Yoder *et al.*, 2010; Stroud & Losos, 2016). In the absence of competing taxa, these events can lead to geographic expansion, which may promote allopatric speciation and decreased extinction. There has recently been an increasing interest in the role of ecological opportunities in the evolutionary origin of biodiversity.

Coevolutionary interactions are one of the most important factors that create new ecological opportunities for rapid diversification (Thompson, 1994; Yoder & Nuismer, 2010; Althoff *et al.*, 2014; Hembry *et al.*, 2014; Hembry & Weber, 2020). For instance, the evolution of plant defenses and insect counter-defenses is known to create new ecological opportunities for both plants (the creation of antagonist-free space) and insects (novel food resources) because the continuous escalation of these traits is likely to increase their respective geographic ranges and thus opportunities for allopatric speciation (i.e. escape-and-radiate; Ehrlich & Raven, 1964; Thompson, 1994; Janz, 2011). Although past studies on coevolutionary diversification have focused on antagonistic interactions, the evolution of mutualistic interactions is also considered to be an important driver for increased diversification rates in many organisms (Thompson, 1994; Yoder & Nuismer, 2010; Hembry *et al.*, 2014).

The evolution of ectomycorrhizal (EcM) symbiosis is considered to be an important evolutionary innovation for both plants and fungi. EcM symbiosis is a ubiquitous mutualistic relationship between plants and fungi in temperate and tropical forest ecosystems that is crucial for survival and growth of both host plants and EcM fungi (Smith & Read, 2008; Tedersoo *et al.*, 2010). Approximately 6000–7000 plant species are involved in EcM symbiosis (Tedersoo & Brundrett, 2017). Most are dominant tree species in temperate and tropical forests, such as those belonging to Pinaceae, Fagaceae, Betulaceae, Dipterocarpaceae, and Myrtaceae (Tedersoo & Brundrett, 2017). The EcM symbiosis also evolved multiple times independently in fungi (Tedersoo *et al.*, 2010; Tedersoo & Smith, 2013). The number of fungal species involved in EcM symbiosis is *c.* 20 000–25 000;

most of these belong to Basidiomycota, specifically to the class Agaricomycetes (Rinaldi *et al.*, 2008; Tedersoo *et al.*, 2010; Tedersoo & Smith, 2013). Recent studies showed that local dominance of EcM trees can be maintained by positive plant–soil feedback in EcM trees (Kadowaki *et al.*, 2018; Liang *et al.*, 2020). Moreover, large-scale biogeography of EcM fungi is reported to be associated strongly with that of host plant species (Sato *et al.*, 2012; Põlme *et al.*, 2013; Tedersoo *et al.*, 2014; van der Linde *et al.*, 2018). These ecological and biogeographic studies indicate a strong coevolutionary relationship between EcM plants and fungi.

An important challenge in this field is to explore what causes the explosive diversification of EcM fungal lineages. Recent phylogenetic studies of Agaricomycetes, the fungal class comprising many EcM fungi and mushroom-forming fungal lineages, have shown that extremely rapid diversification probably occurred in the stem of several EcM fungal clades, but not in any another EcM clade, suggesting that evolutionary diversification of fungal lineages in Agaricomycetes cannot be explained by the evolution of EcM symbiosis alone (Sánchez-García & Matheny, 2017; Sato & Toju, 2019). Other studies suggest that the evolutionary diversification could have been caused by another factor, the evolution of pileate-stipitate and pileate-sessile (i.e. agaricoid) fruitbody forms (Varga *et al.*, 2019; Sánchez-García *et al.*, 2020). However, the character-dependent diversification models used in these studies might oversimplify the driving mechanism of evolutionary diversification, and how the evolution of different fruitbody forms could have created new ecological opportunities remains unknown. Another explanation is that available EcM plants changed substantially through time, which might have led to a temporal heterogeneity of ecological opportunities created by the evolution of EcM symbiosis (Sato & Toju, 2019). In other words, the EcM fungal lineages diverging in the Late Cretaceous might have had opportunities to coevolve with EcM angiosperms (e.g. the development of host recognition systems and repression of plant defenses; Martin *et al.*, 2016), resulting in their expanding into novel niche spaces and the subsequent rapid diversification. However, this hypothesis has never been tested in Agaricomycetes, and thus, how the timing of coevolutionary innovations can influence evolutionary diversification in Agaricomycetes remains to be investigated. Overall, further studies are required to elucidate the evolutionary origin of biodiversity in Agaricomycetes.

This study aims to unravel the driving mechanism of explosive diversification in Agaricomycetes, with special emphasis on testing the hypothesis that the evolutionary diversification was driven by the evolution of EcM symbiosis in the Late Cretaceous. To do this, there is a need to address limitations in previous studies, such as phylogenetic uncertainty, bias caused by confusing cryptic species, and use of oversimplified models. In this study, the historical character transitions of trophic state and fruitbody form were estimated based on molecular phylogenetic trees inferred from fragments of 89 single-copy genes. Moreover, five different approaches, in four of which incomplete taxon sampling was corrected on the basis of the relative richness of fungal operational taxonomic units (OTUs), were used to estimate the temporal dynamics of net diversification rates (i.e. speciation rate minus extinction rate). Based on the results of these analyses, this study tested the hypothesis that the acquisition of EcM symbiosis in the Late Cretaceous, specifically with coevolving angiosperms, facilitated rapid diversification of Agaricomycetes.

Materials and Methods

Taxon sampling

From 2005 to 2021, specimens of 213 macrofungal species were collected from forests in Japan. Small sections of fruitbodies were removed and stored in 99.5% ethanol for molecular analysis, and the remaining sections were dried and preserved as voucher specimens. Dried specimens were deposited in the herbarium at Kyoto University (KYO). DNA samples were also obtained from the specimens deposited in the mycological herbarium of the National Museum of Nature and Science (TNS) and culture collections of the Tottori University Fungal Culture Collection (TUFC).

In addition to 213 new species, 34 reported species (Sato & Toju, 2019) were included in the analysis. The genome sequences of 129 species, including the outgroups (*Calocera cornea* (Batsch) Fr. and *Cryptococcus neoformans* (San Felice) Vuill.), were obtained from the National Center for Biotechnology Information (NCBI) and the Joint Genome Institute (JGI) MycoCosm. In total, 376 species were subjected to the molecular phylogenetic analyses (Supporting Information Table S1).

DNA sequencing procedure

DNA experiments were performed for the 213 newly collected species. Total DNA was extracted from the tissues of dried basidiomes using the cetyltrimethylammonium bromide (CTAB) method, as described previously (Sato & Murakami, 2008). A two-step PCR was performed using the samples, as described previously (Sato *et al.*, 2017). In the first step, fragments of the 104 single-copy genes, ribosomal internal transcribed spacer (ITS) region, and ribosomal large subunit (LSU) region were amplified using the primers listed in Table S2. The primers were designed to contain Illumina sequencing primer regions and 6-mer Ns. The Illumina sequencing adaptors plus 8-bp identifier indices (Hamady *et al.*, 2008) were added in subsequent PCRs using a forward and reverse fusion primer. The PCR conditions for the first and second steps were as described previously (Sato *et al.*, 2017).

After an equal volume of the respective PCR products was pooled, amplicons were purified with a 0.8 × volume of AMPure XP beads (Beckman Coulter, Brea, CA, USA). Then, 450–600-bp long amplicons were excised using 2% E-Gel SizeSelect (Thermo Fisher Scientific, Waltham, MA, USA). The amplicon libraries were sequenced by 2 × 300-bp paired-end sequencing on the MiSeq platform using MiSeq v.3 Reagent Kit (Illumina, San Diego, CA, USA) according to the manufacturer's instructions.

Bioinformatic analyses

BCL2Fastq v.1.8.4 (Illumina) was used for converting the base calls into forward, index1, index2, and reverse Fastq files. Fastq

files were demultiplexed using the FASTQ command of CLAIDENT v.0.2.2019.05.10 (Tanabe & Toju, 2013). The resultant 29 717 186 reads were deposited into the DDBJ Sequence Read Archive (Accession no.: DRA014552). Subsequent processing of the sequencing reads was performed using CLAIDENT, as described previously (Sato *et al.*, 2017).

Molecular phylogenetic analyses

Removal of nonorthologous sequences and identification of exon–intron boundaries were performed as described previously (Sato *et al.*, 2017). The third codon positions were removed to avoid the risk of substitution saturation. Sequences of 10 single-copy genes (FG740, FG866, MS400, FG621, FG821, FG735, FG487, FG692, FG708, and MS485) were not used for subsequent analyses because only a few samples could be sequenced. Sequences of five single-copy genes (FG556, FG507, FG863, MS241, and FG665) were removed because their congruence with other loci was not strongly supported by 'Congruence among distance matrices' (CADM) test (Campbell *et al.*, 2011), which was performed using 'CADM.global' in the APE package (Paradis *et al.*, 2004) of R v.4.0.2 (R Development Core Team, 2020). Thus, 89 single-copy genes were phylogenetically analyzed.

Molecular phylogenetic analyses based on the maximum likelihood (ML) method were performed on the concatenated sequences of 89 loci using RAXML v.8.2.4 (Stamatakis, 2006). The searches were repeated 93 times using random sequence addition to generate starting trees. For the analysis, the concatenated data set was partitioned by gene and codon position (178 partitions). Parameters of the GTR Gamma model were estimated separately for each partition according to model selection by the Akaike information criterion (AIC); the smallest AIC value indicates the most appropriate model given the data using the KAKUSAN4 program (Tanabe, 2011). The outgroups (i.e. *C. cornea* and *C. neoformans*) were used for rooting the ingroup. Bootstrap support (BS) values were calculated from 500 standard bootstrap replications, as implemented in RAXML.

Bayesian molecular clock analysis was performed using BEAST v.2.6.6 (Bouckaert *et al.*, 2014) with an uncorrelated lognormal relaxed clock using seven fossil calibration points (Table S3). The analysis comprised 10 simultaneous runs, sampled at every 100 000th generation for 50 million generations with an initial 10% burn-in, assuming a Yule speciation model for the tree prior. The most appropriate substitution models for 188 partitions were selected by KAKUSAN4. The final log and tree files were combined in BEAST2 LOGCOMBINE (Bouckaert *et al.*, 2014), and the convergence of independent runs and effective sample size (ESS > 100) were checked in TRACER v.1.6. TREEANNOTATOR v.1.6.1 was used to sum the trees after burn-in for the 50% majority-rule consensus 'maximum clade credibility tree' with 'mean heights' for node heights.

Estimation of historical patterns of states

Historical patterns of trophic states (i.e. EcM vs non-EcM) and fruitbody types (agaricoid vs nonagaricoid) in phylogenies were inferred using stochastic mutational mapping (SIMMAP; Bollback, 2006). Ancestral states were evaluated across nodes of the Bayesian ultrametric tree by generating 1000 stochastic character maps with the 'make.simmap' function of PHYTOOLS v.1.0-3 in R package (Revell, 2012). For an illustrative purpose, the functions 'setMap' and 'densityMap' of PHYTOOLS were also used. The trophic state and fruitbody type of each taxon were identified on the basis of the FUNGALTRAITS database (Põlme *et al.*, 2020; Table S1). For agaricoid fruitbody, two definitions were used defined as both of pileate-stipitate and pileate-sessile (agaricoid s.l.) or pileate-stipitate only (agaricoid s.s.). Trophic states were identified at the species level for fungal genera for which different trophic states were known (see details in Methods S1).

Estimation of OTU richness

To estimate OTU richness (i.e. a proxy for species richness) of respective taxa in Agaricomycetes, ITS sequences of Agaricomycetes with sequence lengths ranging from 400 to 1200 bp were obtained from the NCBI database. To reduce the effect of base-calling errors, sequences with > 1% of their total length being ambiguous bases (N) were excluded. A total of 176 020 sequences were clustered into OTUs at sequence identity ≤ 97 using CLAIDENT (30 991 OTUs). The ITSX software (Bengtsson-Palme *et al.*, 2013) was also used to extract OTUs that included sequences of fungal ITS1 regions (29 666 OTUs). After taxonomic assignment of the OTUs using CLAIDENT was complete, OTU richness for each fungal taxon was inferred based on the number of accessions and observed OTU richness using iNEXT in R (Hsieh *et al.*, 2016; Table S4). The obtained values were used in subsequent analyses for estimating net diversification rates.

Estimation of net diversification rates

In this study, net diversification rates (i.e. speciation rate minus extinction rate) were evaluated. However, the methodologies used for estimating diversification rates are controversial (May & Moore, 2016; Moore *et al.*, 2016; O'Meara & Beaulieu, 2016; Rabosky *et al.*, 2017; Meyer & Wiens, 2018; Rabosky & Benson, 2021). To reduce methodological artifacts, five types of methods were used.

First, evolutionary diversification was inferred using Bayesian Analyses of Macroevolutionary Mixtures (BAMM), which uses the Reversible Jump MCMC method to detect variation in diversification rate over time and between lineages (Rabosky *et al.*, 2014). The function 'setBAMMpriors' in the R package BAMMTOOLS (Rabosky *et al.*, 2014) was used to generate a prior block that matched the scale of the data. Then, BAMM was applied to the Bayesian ultrametric tree with eight chains for 25 000 000 generations, sampling every 10 000th generation. BAMM was applied not only to the ultrametric tree obtained in this study but also to the megaphylogeny (i.e. tree no. 8) obtained by Varga *et al.* (2019). To address incomplete and biased taxon sampling, taxon-specific sampling fraction for each fungal taxon (Table S5) was incorporated in the analysis using three schemes (see details in Methods S1). This study focuses on the method using estimated OTU richness to

address numerous cryptic species and synonymous species in Agaricomycetes (Hawksworth, 2001; Sato *et al.*, 2020; Cao *et al.*, 2021). Incomplete taxon sampling was also corrected using the stochastic polytomy resolving program TACT (Chang *et al.*, 2020) by placing the unsampled taxa onto the background tree (called the output tree; hereafter, 'TACT tree'). For the previous megaphylogeny, only the TACT method was used (called as the Varga TACT tree, hereafter). After assessing the convergence and adequate ESS (> 100) of all parameters using TRACER, the BAMMTOOLS package was used to remove 20% burn-in and plot the net diversification rate through time. Among the distinct rate shift configurations (1513, 1412, and 3041 in the original tree, TACT tree, and Varga TACT tree, respectively), the configuration of rate shifts with the highest posterior probability was plotted using the 'getBestShiftConfiguration' function of BAMMTOOLS.

Second, the temporal trend of net diversification rates was captured by modeling evolutionary diversification using stepwise AIC (MEDUSA; Alfaro *et al.*, 2009) program, a stepwise AIC algorithm that fits a series of birth-death models to ultrametric trees. This program integrates divergence times obtained from the phylogenetic tree with taxonomic richness data to detect clade-specific diversification processes and, thus, is likely to be more robust for incomplete taxon sampling than BAMM analysis (Alfaro *et al.*, 2009; Chang *et al.*, 2020). Here, the 'medusa' function of GEIGER v.2.0.7 in R (Pennell *et al.*, 2014) was used to detect diversification rate shifts. Taxon-specific sampling fraction was incorporated in the analysis using three schemes as described in the BAMM analysis.

Third, evolutionary diversification was evaluated using the method-of-moments estimator (Magallon & Sanderson, 2001), in which net diversification is estimated through the relationship between clade age and contemporary species richness. This method is superior in terms of the robustness of incomplete taxon sampling in phylogenies (Moore *et al.*, 2016; Meyer & Wiens, 2018; Chang *et al.*, 2020). To avoid the artifacts caused by the occurrence of cryptic and synonymous species, estimated OTU richness (Table S4) was used as a proxy for contemporary taxon richness. The stem and crown ages of each fungal taxon were calculated based on the ultrametric tree obtained with BEAST2. Then, the net diversification rates of respective fungal taxa were estimated using the 'bd.ms' function of GEIGER, based on crown age, stem age, and mean of crown and stem ages. This study focused on net diversification rates calculated based on the mean of crown and stem ages to examine the relationship between historical character changes and diversification rate shifts. Notably, the estimated net diversification rates appeared to have a strong negative correlation with clade ages when low ε values (i.e. extinction rate as a fraction of speciation rate) were used (Fig. S1). Because the overestimation of diversification rates in younger clades is a known problem (Rabosky & Benson, 2021), extremely high ε values (0.9, 0.99, and 0.999) were used in this study to reduce overestimation bias.

Fourth, the DR statistic (Jetz *et al.*, 2012), an approach to inferring recent speciation rates for all tips in phylogeny (tip rates), was used. This analysis was performed to address the issue that deep temporal trends in diversification rate shifts could not be reliably identified by the phylogeny of extant species (Louca & Pennell, 2020), because estimates of tip rates are known to be relatively robust to this issue (Louca & Pennell, 2020). The original tree was used in this analysis, for which taxon-specific sampling fraction was not incorporated. Similarly, the net diversification rates of all tips were calculated for the original tree of this study using the 'getTipRates' command of the BAMMTOOLS package. The tip rates were regressed against the focal states, including the trophic state (EcM with the Late Cretaceous origin, other EcM, and non-EcM) and fruitbody form (pileate-stipitate, pileate-sessile and nonagaricoid), using the 'lm' function in R. Thereafter, the AIC values were compared.

Last, the impact of focal binary traits on net diversification rates was assessed using the binary state speciation–extinction (BiSSE) and Hidden State Speciation and Extinction (HiSSE) models. The BiSSE model is widely used, but simplistic assumptions may cause spurious assignments of diversification rate differences between focal characters (Rabosky & Goldberg, 2015). The HiSSE model addresses this problem by assuming the existence of unobservable (hidden) characters that could impact diversification rates (Beaulieu & O'Meara, 2016). These models were applied to the original and TACT trees of this study and the Varga TACT tree using the 'hisse.old' and 'hisse.null4.old' functions of the HISSE package of R (Beaulieu & O'Meara, 2016). For the Varga TACT tree, apparently misidentified taxa were precluded from the analysis using 'drop.tip' function of APE in R. For the original tree, the state-specific sampling fractions calculated based on estimated OTU richness (Table S1) were used to address incomplete taxon sampling. For TACT trees, species belonging to the genera in which EcM and non-EcM fungi were mixed were precluded. Then, four models were tested: a character-independent diversification model (Vasconcelos *et al.*, 2022) with two (CID-2) or four (CID-4) hidden states, a BiSSE model, and a HiSSE model with four hidden states. In these models, the net turnover rates (speciation rate plus extinction rate) were allowed to change according to the state, whereas the net eps rates (extinction fraction) were set to be equal to simplify the model. The focal characters were the presence or absence of EcM symbiosis and agaricoid fruitbody (two definitions). The character-transition models, all rate different (ARD), equal rate (ER), and unidirectional evolution toward EcM (UD) were included. Consequently, the AIC values of 17 models were compared. Thereafter, a likelihood ratio test was performed to test the null hypothesis that both of turnover and eps rates did not change according to the focal state (i.e. equal net diversification rates). Furthermore, to visualize the relationship between ancestral character and net diversification rate, the Bayesian MCMC implementation of the most appropriate model was run for the ultrametric tree, using the REVBAYES software (Höhna *et al.*, 2016; see details in Methods S1).

Results

Phylogenetic relationships in Agaricomycetes

Maximum likelihood (Fig. S2) and Bayesian (Fig. S3) trees inferred from fragments of 89 single-copy genes provided useful

information about the phylogenetic relationship of the Agaricomycetes. The orders Cantharellales, Sebacinales, and Auriculariales were sisters to the clade comprising the remaining fungal orders with 88% BS. Phallomycetidae, the clade comprising the orders Gompales, Hysterangiales, Geastrales, and Phallales, was monophyletic and sister to Trechisporales with 95% BS. Agaricomycetidae, a clade comprising Agaricales, Atheliales, Amylocorticiales, and Boletales, was monophyletic with 75% BS. The orders Polyporales, Thelephorales, Russulales, Corticiales, and Gloeophyllales formed a moderately supported clade (BS = 69%). Most fungal orders in Agaricomycetes were recovered as monophyletic with high BS (100%, 100%, 100%, 100%, 100%, 100%, 100%, 99%, 99%, 94%, and 84% BS for Sebacinales, Auriculariales, Phallales, Hymenochaetales, Thelephorales, Russulales, Gloeophyllales, Boletales, Geastrales, Gomphales, and Polyporales), except for Cantharellales, Agaricales, and Atheliales. All EcM families in Cantharellales (Cantharellaceae, Hydnaceae, and Clavulinaceae) formed a large monophyletic clade with 100% BS and were sister to non-EcM families in Cantharellales (Botryobasidiaceae and Tulasnellaceae) with 70% BS. The clade comprising these taxa was paraphyletic to the non-EcM clade comprising Ceratobasidiaceae, contradicting the monophyly of Cantharellales. Within Phallomycetidae, Hysterangiales was recovered as sister to Gomphales (BS = 95%). Within Agaricales, Agaricales s.s. (see Fig. S2) was monophyletic with 87% BS. Moreover, the fungal taxa with brownish-to-rusty basidiospores (Cortinariaceae, Bolbitiaceae, Inocybaceae, Crepidotaceae, Tubariaceae, Hymenogastraceae, and Strophaliaceae) formed a monophyletic clade with 99% BS. Within Atheliales, the EcM genus *Piloderma* (Atheliaceae) and the non-EcM genus *Fibularhizoctonia* (Atheliaceae) formed a monophyletic clade with 99% BS that was polyphyletic to the non-EcM genus *Athelia* (Atheliaceae). Within Polyporales, Sparassidaceae was sister to Fomitopsidaceae and together the two formed a monophyletic clade comprising brown-rot fungi with 96% BS. The monophyly of most families in Agaricomycetes was supported with high BS, excluding Hymenogastraceae, Tubariaceae, Crepidotaceae, Bolbitiaceae, Tricholomataceae, Lyophyllaceae, Hygrophoraceae, Atheliaceae, Sclerodermataceae, and Meruliaceae (also see a taxonomic revision proposed for several families in Table S1).

The crown and stem ages of respective orders were similar to but somewhat older than those suggested in other studies, presumably due to the differences in the tree topology, taxon sampling, and number of fossil calibration points. The monophyletic orders Gloeophyllales, Thelephorales, Russulales, and Polyporales appeared to have Middle to Late Jurassic origins, whereas Agaricales, Boletales, and Hymenochaetales appeared to have an Early Jurassic origin.

Evolution of EcM and agaricoid fruitbody in Agaricomycetes

Most of the EcM fungal clades were shown to be monophyletic with high BS (Figs 1a, S2, S3), although the phylogenetic placements of some EcM fungal groups, such as *Phaeocollybia* (Hymenogastraceae) and *Catathelasma* (Biannulariaceae), remain ambiguous. Among the transition rate models of EcM symbiosis, the UD model was the most appropriate (Table 1). The acquisition of EcM symbiosis was inferred to occur 27 times independently.

The timing of EcM symbiosis evolution differed substantially between EcM fungal clades (Fig. 1a). The EcM Cantharellales clade had the most ancient EcM origin, dated to the Early Triassic. The Bankeraceae clade was the second oldest EcM fungal clade, dated to the Early Cretaceous. The EcM origins of *Sebacina*, Sclerodermatineae, *Amanita*, and Suillineae were dated to the Middle Cretaceous. The EcM origins of Thelephoraceae, *Cortinarius*, Russulaceae, *Inocybe*, and Boletaceae were dated to the Late Cretaceous. The EcM origins of Gomphaceae, *Hygrophorus*, *Hebeloma*, Paxillineae, and *Entoloma* were estimated to be in the Early Paleogene, although caution should be exercised in interpreting the EcM origin of Gomphaceae, in which trophic states remain to be examined for several taxa. The EcM origins of the remaining clades were unclear because of the lack of non-EcM sister (*Tricholoma* and Hydnangiaceae), insufficient taxon sampling (*Albatrellus*, *Catathelasma*, *Descolea*, *Lyophyllum*, *Phaeocollybia*, and *Piloderma*), and low sequencing quality (*Coltricia*).

Among the transition rate model of agaricoid fruitbodies, the ARD and ER models showed almost the same AIC scores, regardless of the agaricoid definition (Table 1), not strongly supporting directional evolution. The acquisition and loss of agaricoid s.l. fruitbodies were inferred to occur repeatedly (Fig. 1b); the acquisition occurred between the Late Triassic and the Early Jurassic in the stem of the major members of Agaricales, between the Early and Late Jurassic in the stem of the clade comprising Cantharellaceae and Hydnaceae, between the Late Jurassic and Early Cretaceous in the stem of Bankeraceae, between the Early and middle Cretaceous in the stem of Boletineae, and in the Late Cretaceous in the stem of Russulales. However, relatively large errors were present in estimating the timing of evolution of agaricoid forms because of trait loss and phylogenetic uncertainty in some agaricoid clades (e.g. Agaricales).

Evolutionary diversification in Agaricomycetes

Estimation of OTU richness for Agaricomycetes showed 45 469 OTUs, of which 19 895 were EcM fungi (Table S4; Fig. S4), corroborating high biodiversity of mushroom-forming fungi and EcM fungi.

The net diversification rate estimated by BAMM differed between EcM and non-EcM fungi, rather than between agaricoid (agaricoid s.l.) and nonagaricoid fungi, even within the clade of Agaricomycetidae in which agaricoid fungi are dominant (Fig. 2). This pattern persisted regardless of the agaricoid definition (data not shown). The diversification rate in EcM fungi rapidly increased during the Late Cretaceous but changed little in non-EcM fungi. In this study, the difference in net diversification rates between agaricoid and nonagaricoid was most distinct in the TACT tree, but less clear than that between EcM and non-EcM fungi. A substantial increase in net diversification rates occurred in the stems of EcM fungal clades that diverged in the Late Cretaceous, such as Boletaceae, *Inocybe*, *Cortinarius*,

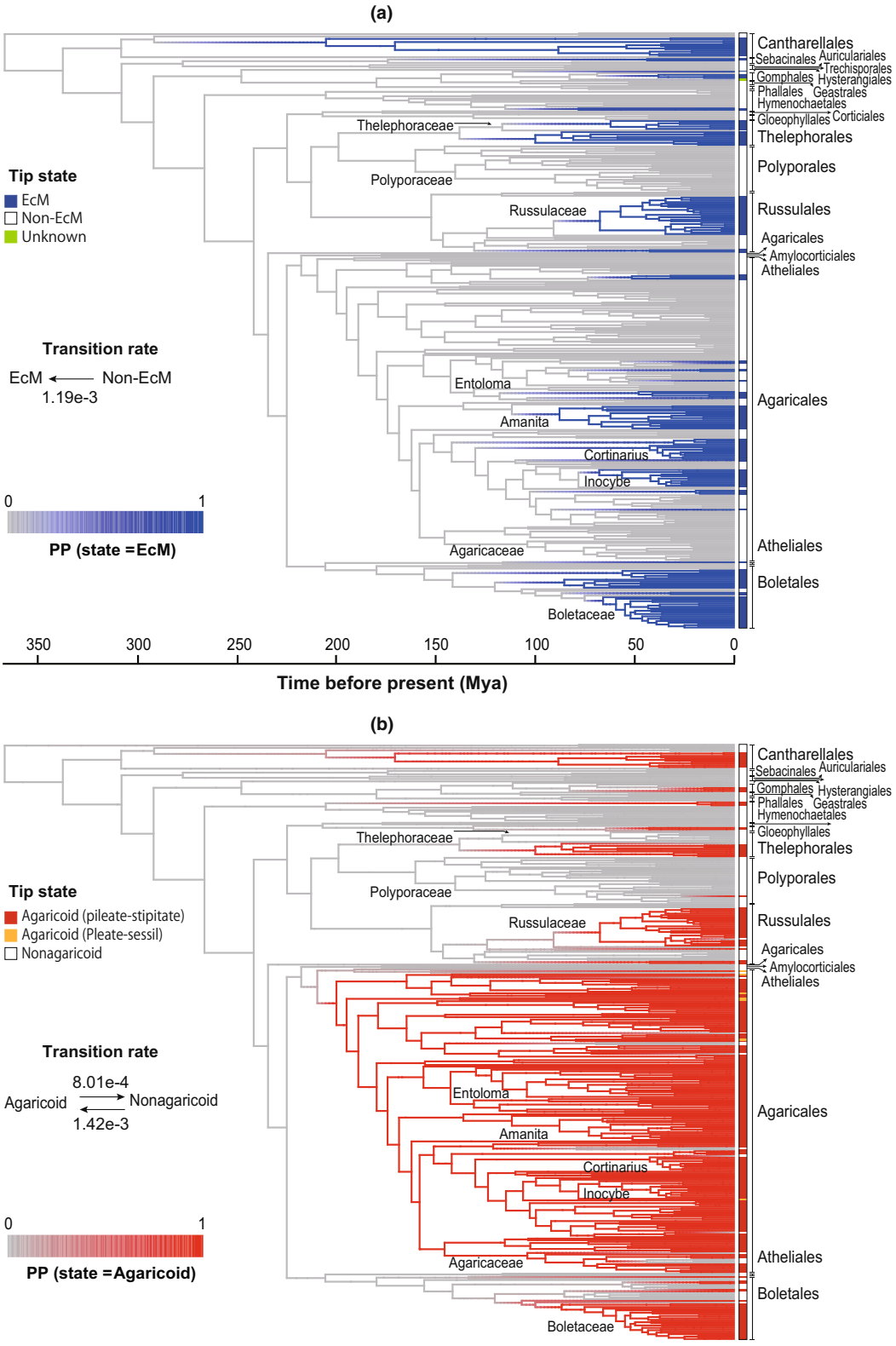

Fig. 1 Historical character transition of (a) ectomycorrhizal (EcM) symbiosis and (b) agaricoid s.l. (pileate-stipitate and pileate-sessile) fruitbody in Agaricomycetes estimated using stochastic mutational mapping (SIMMAP). Branch colors represent the posterior probability of focal states along the edges of the tree. Branch lengths indicate time of divergence. Focal tip states and character-transition rates are listed to the right of the phylogeny.

Russulaceae, and Thelephoraceae, according to BAMM (Figs 3a, 4) and MEDUSA (Fig. 3b). These major rate shifts were observed, regardless of the methods to address incomplete taxon sampling (Figs 3, 4, S5–S9). However, the increased diversification rate in Thelephoraceae was not distinct in MEDUSA (Fig. 3b) and BAMM for the TACT tree (Fig. 4a), presumably due to the

Table 1 Model comparison of character transition in Agaricomycetes based on the Akaike information criteria (AIC).

Model	$\log_e$ L	AIC	ΔAIC
ECM			
ARD	−105.0	214.0	1.9
ER	−106.0	214.1	2.0
UD	−105.0	212.1	
Agaricoid s.l.			
ARD	−109.8	223.6	0.0
ER	−110.8	223.6	
Agaricoid s.s.			
ARD	−123.0	250.0	1.9
ER	−123.0	248.1	

Log likelihood ($\log_e$ L), AIC score, and AIC difference between a model with lowest AIC score (most appropriate model) and focal model (ΔAIC) are shown. Here, two binary states, ectomycorrhizal (EcM) or not vs agaricoid fruitbody or not, were considered. For agaricoid, two definitions, agaricoid s.l. (pileate-stipitate and pileate-sessile) and agaricoid s.s. (pileate-stipitate only) were prepared.

undersampling of taxa. Moreover, the Varga TACT tree showed many small-scale rate shifts and an exaggerated rate shift in the stems of Ceratobasidiaceae and Atheliaceae (Fig. 4b), presumably due to the increase in statistical power with increasing species number and the undersampling of fungal taxa with inconspicuous fruitbodies. A slight increase in diversification rates was seen in several clades, including *Amanita* (Figs 3, 4a, S8, S9a), *Tricholoma* (Figs 4a,b, S8a,b), Polyporaceae (Figs 3, 4, S8, S9), *Entoloma* (Figs 3, 4, S8, S9a), and Agaricaceae (Figs 3, 4, S8, S9). Overall, the different approaches of BAMM and MEDUSA provided similar results, supporting the explosive diversification of EcM fungi in the Late Cretaceous.

Results of the method-of-moment estimator were similar to those of BAMM, specifically in higher ε values. For instance, higher diversification rates were inferred for the EcM fungal clades that diverged in the Late Cretaceous (Fig. 5; Table S6). Nevertheless, high diversification rates observed in some young clades, such as *Agaricus*, *Hebeloma*, *Gymnopus*, *Armillaria*, and Stereaceae, with lower ε values, were not reliable because the values changed drastically depending on the ε value (Fig. 5; Table S6). In addition, decreased diversification rates were indicated for Phallales, Nidulaceae, Cantharellales, Auriculariales, Schizoporaceae, and Gloeophyllaceae (Fig. 5; Table S6). Consequently, the increased diversification rates of EcM fungi in the Late Cretaceous were supported by the method-of-moment estimator with high ε values.

The DR statistic and BAMM tip rates were explained by the trophic state, rather than the fruitbody form (Fig. 6). High tip rates were indicated in the EcM fungal clades diverging in the Late Cretaceous.

The analysis of trait-dependent diversification corroborated the rapid diversification of EcM fungi in the Late Cretaceous. Based on model comparison, the CID models were rejected in favor of the HiSSE model of EcM states in all trees (Table 2). The analysis rejected agaricoid state-dependent diversification in favor of EcM state-dependent diversification, regardless of the agaricoid definition (Table 2). Among EcM state-dependent diversification, the HiSSE model with UD transition was as the most appropriate model, except for the Varga TACT tree (Table 2). The most appropriate for the Varga TACT tree was the HiSSE model with ARD transition, in which the transition rate from non-EcM to EcM was > 10 times higher than that of reversal evolution. The HiSSE model, assuming equal net diversification rates between EcM and non-EcM fungi, was rejected in all the trees by the likelihood ratio test ($P < 0.001$). RevBayes analysis revealed that the rapid increase in diversification rates occurred around the stem of the EcM fungal taxa that diverged at the Late Cretaceous, except for Thelephoraceae, the most undersampled taxa (Fig. 7). Consequently, the diversification rates estimated with the HiSSE/EcM model were found to support the explosive diversification of EcM fungal taxa in the Late Cretaceous.

Discussion

The results of this study have important implications for understanding the evolution and evolutionary diversification of Agaricomycetes. The unidirectional evolution of EcM symbiosis was inferred to occur multiple times in Agaricomycetes. The evolution of EcM symbiosis occurring in the Late Cretaceous was shown to be the key innovation event that led to rapid diversification. Although several methodological issues remain to be addressed, these findings largely support the hypothesis that explosive diversification could have been driven by the evolution of EcM symbiosis in the Late Cretaceous.

The results of molecular phylogenetic inference provide new insight into the phylogenetic relationship of Agaricomycetes. The results improved the phylogenetic resolution of Cantharellales and Phallomycetidae, which were poorly resolved in megaphylogenies (Varga *et al.*, 2019; Sánchez-García *et al.*, 2020). For instance, the EcM fungal taxa belonging to Cantharellales were suggested to form a monophyletic clade. However, caution should be exercised in interpreting the EcM origin of this clade because the phylogenetic placements of some non-EcM genera in Cantharellales, such as *Multiclavula* and *Sistotrema*, remain to be investigated. The fungal taxa with brownish-to-rusty basidiospores in Agaricales and brown-rot fungi within Polyporales were monophyletic. Overall, these findings have important implications for understanding the phylogenetic relationships in Agaricomycetes.

The results of this study elucidate the evolutionary patterns of EcM symbiosis in Agaricomycetes. The results of model comparison suggest that the evolution of EcM symbiosis is unidirectional (Tables 1, 2), consistent with others (Tedersoo & Smith, 2013; Sato & Toju, 2019). However, caution is needed in interpreting these results, because unknown information, specifically about the trophic states and phylogenetic placements of *Gloeocantharellus* and *Ramaria*, could affect the results. The number of independent events inferred in this study (i.e. 27 times) is likely underestimated, because the evolution of EcM symbiosis was inferred to occur at least 37 times in Agaricomycetes (Tedersoo *et al.*, 2010; Tedersoo & Smith, 2013). Indeed, some minor

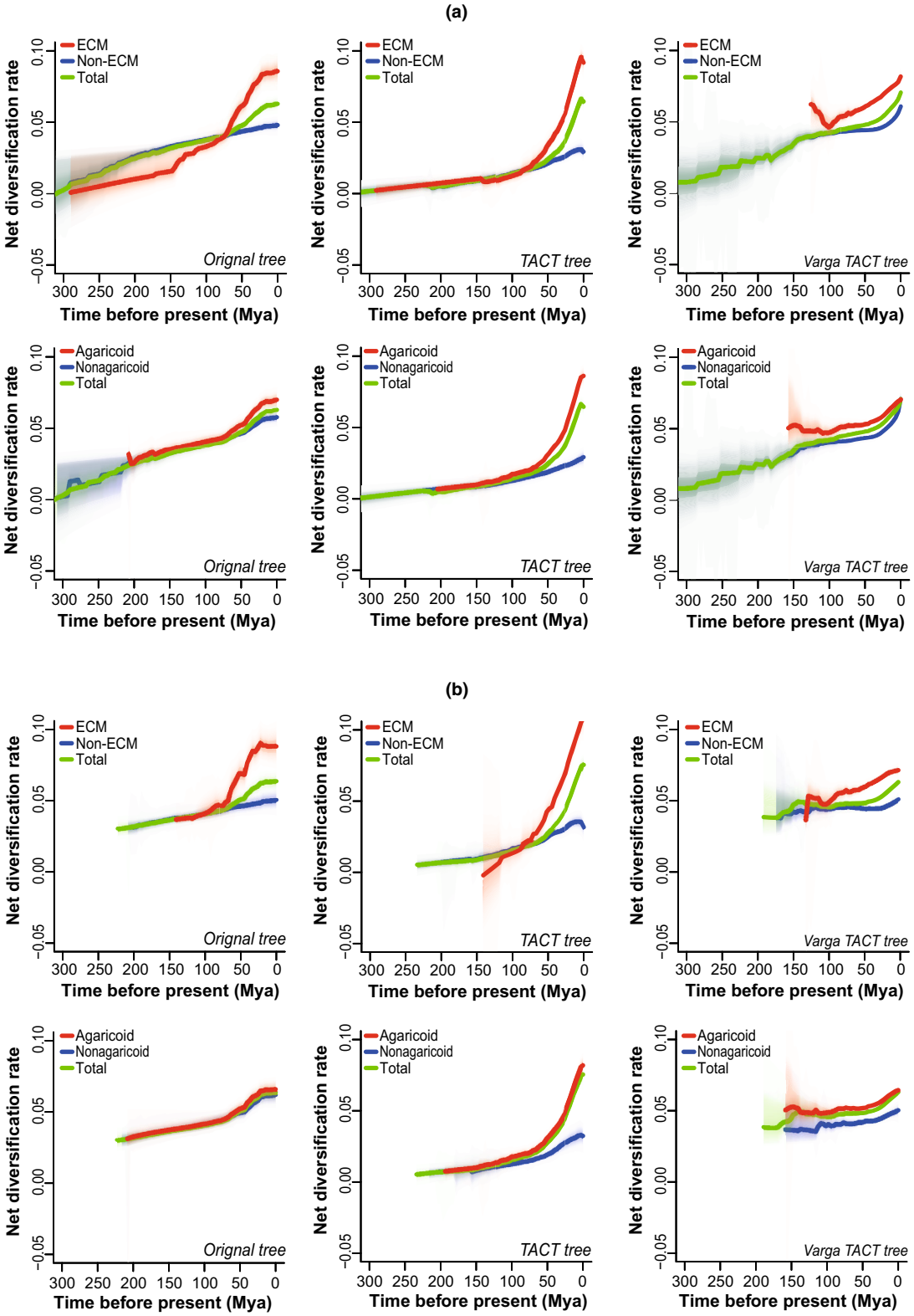

Fig. 2 Rate-through-time plot of net diversification rates (i.e. speciation rate minus extinction rate) in (a) Agaricomycetes and (b) Agaricomycetidae estimated by the Bayesian Analyses of Macroevolutionary Mixtures (BAMM). The patterns are compared between ectomycorrhizal (EcM) vs non-EcM (upper) and agaricoid s.l. (pileate-stipitate and pileate-sessile) fruitbody vs nonagaricoid fruitbody (lower) in the original tree of this study with the taxon-specific sampling fraction (left), the TACT tree of this study (middle), and the TACT tree of Varga *et al*. (2019; right).

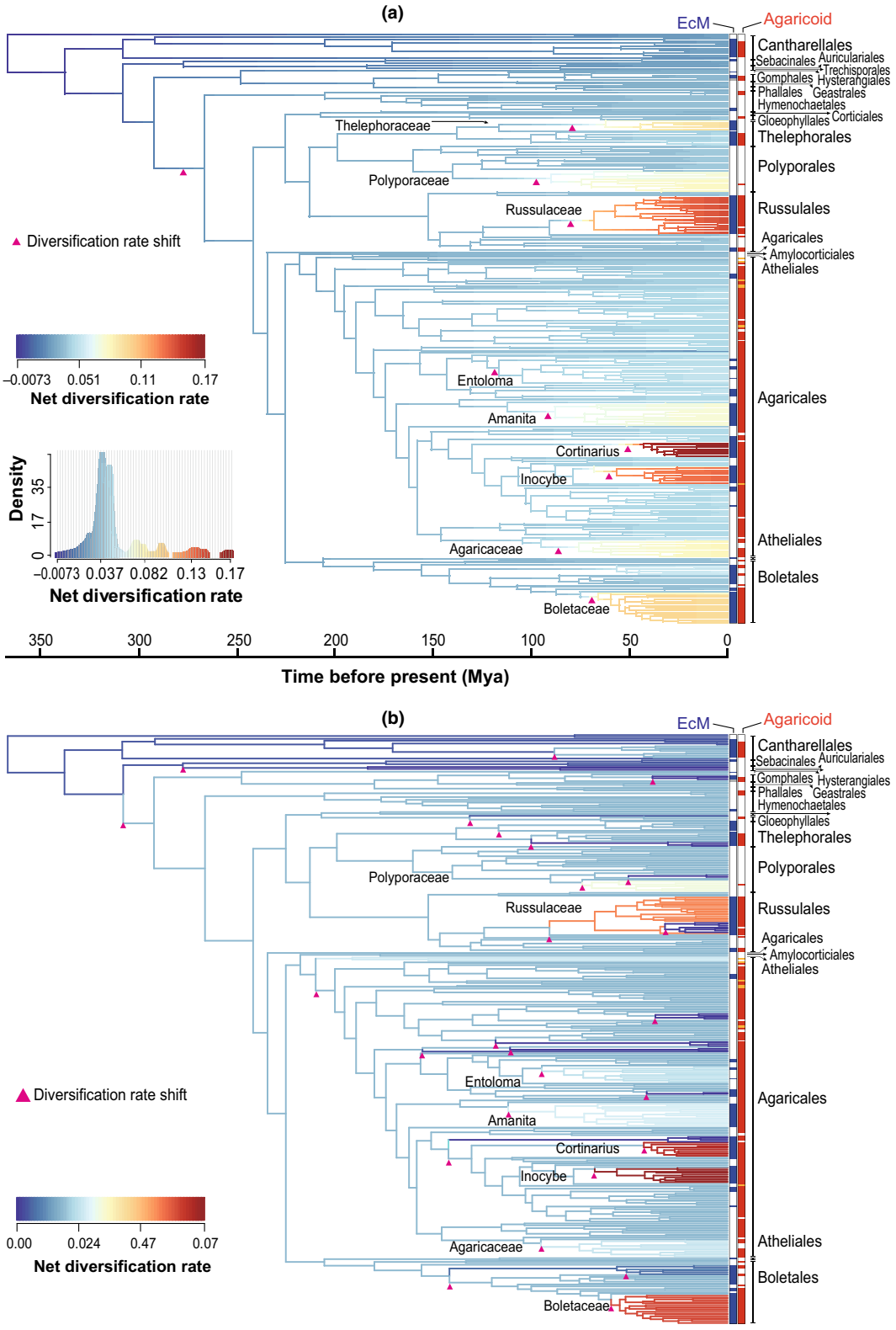

Fig. 3 Dynamics of net diversification rates (i.e. speciation rate minus extinction rate) in Agaricomycetes estimated using (a) Bayesian Analysis of Macroevolutionary Mixtures (BAMM) and (b) modeling evolutionary diversification using stepwise AIC (MEDUSA), in which taxon-specific sampling fraction is calculated based on estimated richness of operational taxonomic units (OTUs) in the NCBI database. Branch colors represent relative net diversification rates along the edges of the tree. A triangle depicts the significant rate shift point suggested by the rate shift configuration with the maximum a posteriori probability. Branch length indicates divergence time. Focal states of extant species are listed to the right of the phylogeny. For trophic state, ectomycorrhizal (EcM), non-EcM, and unknown state are shown in blue, white, and gray, respectively. For fruitbody form, pileate-stipitate, pileate-sessile, and nonagaricoid are shown in red, orange, and white, respectively.

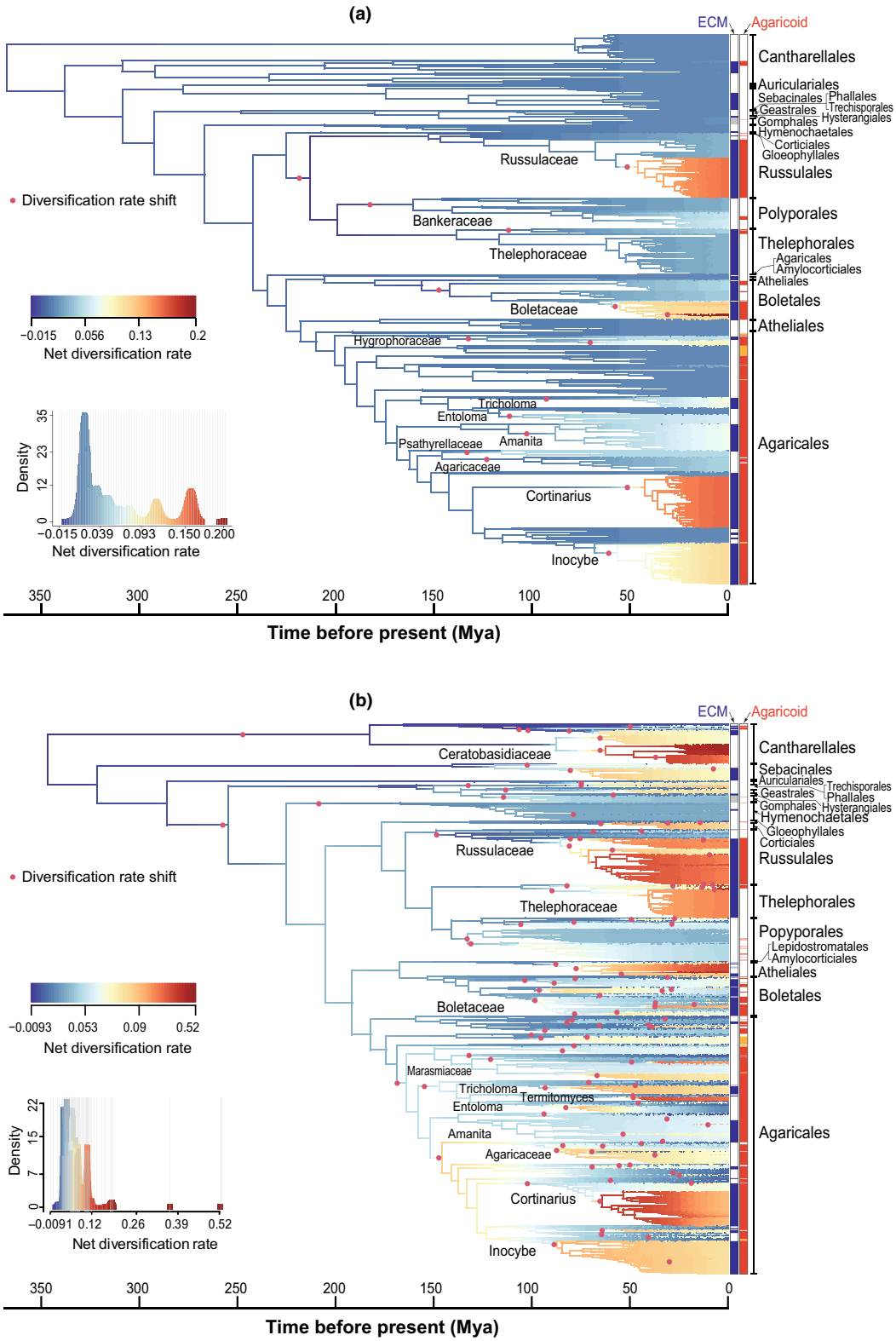

Fig. 4 Dynamics of net diversification rates (i.e. speciation rate minus extinction rate) in Agaricomycetes estimated using Bayesian Analysis of Macroevolutionary Mixtures (BAMM) for the TACT tree of (a) this study and (b) Varga *et al*. (2019). Branch colors represent relative net diversification rates along the edges of the tree. A closed circle depicts the significant rate shift point suggested by the rate shift configuration with the maximum a posteriori probability. Branch length indicates divergence time. Focal states of extant species are listed to the right of the phylogeny. For trophic state, ectomycorrhizal (EcM), non-EcM, and unknown state are shown in blue, white, and gray, respectively. For fruitbody form, pileate-stipitate, pileate-sessile, and nonagaricoid are shown in red, orange, and white, respectively.

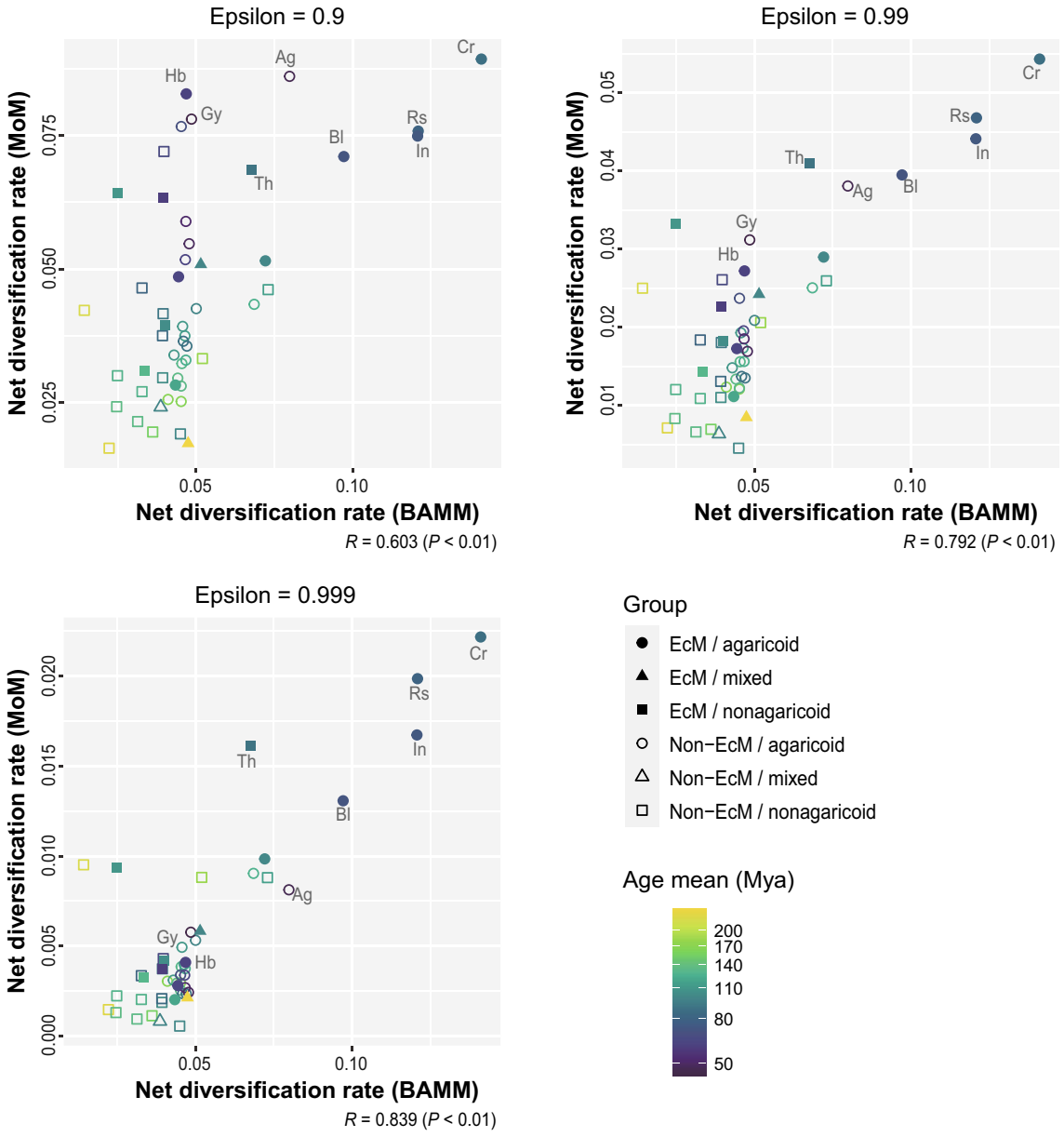

Fig. 5 Relationship between net diversification rates (i.e. speciation rate minus extinction rate) of fungal taxa belonging to Agaricomycetes estimated by the Bayesian Analysis of Macroevolutionary Mixtures (BAMM) and method-of-moments (MoM) estimator. Net diversification rates of BAMM are estimated using the original tree of this study with the taxon-specific sampling fractions. Net diversification rates of MoM are estimated by changing the value of ε (extinction rates divided by speciation rates). Colors indicate clade ages (mean of crown and stem ages). Symbols represent trophic state (ectomycorrhizal (EcM) or not) and fruitbody type (agaricoid or not). Abbreviations correspond to the fungal taxa (*Cortinarius* (Cr), Russulaceae (Rs), *Inocybe* (In), Boletaceae (Bl), Thelephoraceae (Th), *Agaricus* (Ag), *Hebeloma* (Hb), and *Gymnopus* (Gy)). Obtained values of clade ages, net diversification rates, and OTU richness are shown in Supporting Information Table S6.

EcM fungal lineages were lacking in this study, such as *Amphinema-Tylospora* (Atheliales), *Byssocorticium* (Atheliales), and *Austropaxillus* (Boletales). Moreover, the fungal genera whose primary lifestyles are not EcM, such as *Serendipita*, *Tulasnella*, and *Ceratobasidium* (Põlme *et al.*, 2020), were not treated as EcM in this study. However, the number of EcM origination events in Agaricomycetes might have been overestimated due to phylogenetic uncertainty. Although the phylogenetic placements of missing taxa could affect the results, some EcM fungal taxa were shown to form large EcM fungal clades, such as the EcM Cantharellales (*Cantharellus*, *Clavulina*, and *Hydnum*), Thelephoraceae (*Thelephora*, *Tomentella*, and *Pseudotomentella*), and Bankeraceae (*Bankera*, *Phellodon*, *Polyzellus*, *Boletopsis*, and *Sarcodon*; Figs S2, S3). Consequently, the EcM symbiosis is considered to have evolved in Agaricomycetes ≥ 30 times.

The findings of this study suggest that the evolutionary timing of EcM symbiosis coincided between Agaricomycetes and plants. For instance, the EcM Cantharellales was shown to have an ancient EcM origin, dated to the Early Triassic, somewhat similar to the radiation of Pinaceae, the plant family with the

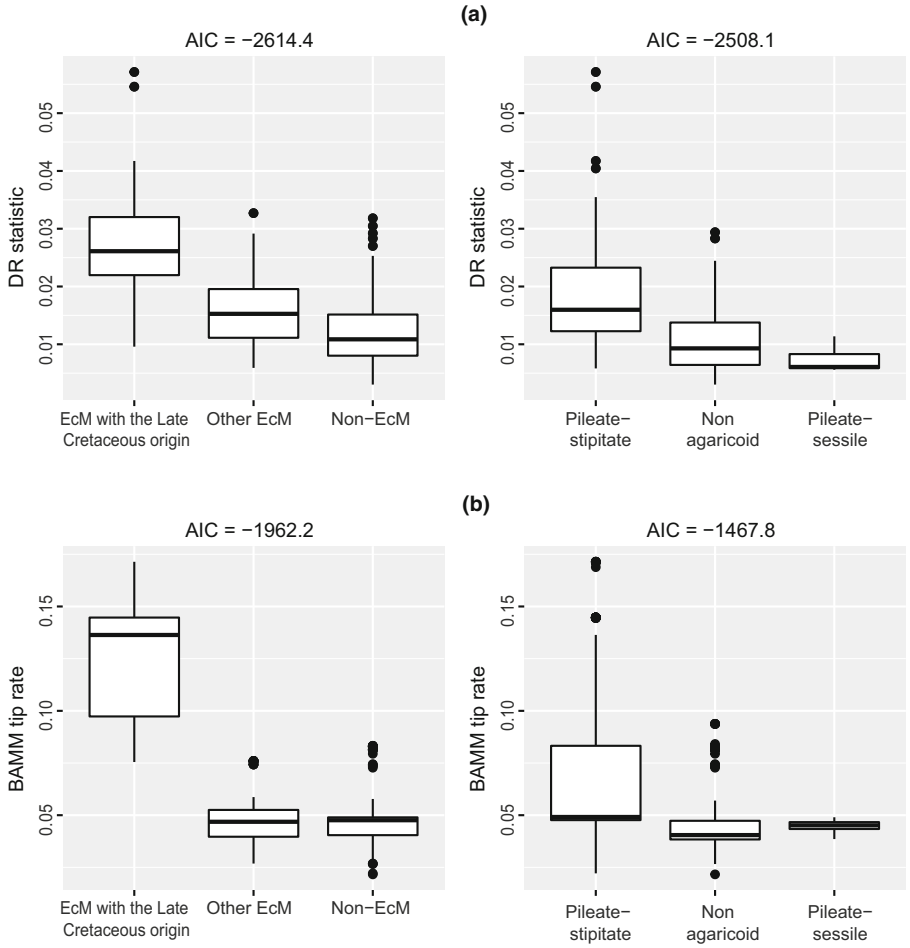

Fig. 6 Boxplot of species-specific recent tip rates in Agaricomycetes estimated by (a) the DR statistic and (b) the Bayesian Analysis of Macroevolutionary Mixtures (BAMM). The solid horizontal bars show the median, the edges of the boxes show the lower and upper quartiles, whiskers show the extent of values up to 1.5 times the interquartile range, and the closed circles show the outliers beyond this limit. Akaike information criteria (AIC) scores of linear regression between tip rates and focal states, including trophic state (ectomycorrhizal (EcM) with the Late Cretaceous origin, other EcM, and non-EcM) and fruitbody form (pileate-stipitate, pileate-sessile, and nonagaricoid), are shown above the boxplot.

most ancient EcM origin (Zanne *et al.*, 2014; Tedersoo & Brundrett, 2017; Lutzoni *et al.*, 2018). The EcM origins of Thelephoraceae, *Cortinarius*, Russulaceae, *Inocybe*, and Boletaceae were dated to the Late Cretaceous, largely consistent with the divergence ages of EcM angiosperm families, specifically those of Fagales (Zanne *et al.*, 2014; Larson-Johnson, 2016; Tedersoo & Brundrett, 2017; Lutzoni *et al.*, 2018), underlying the simultaneous evolution of these fungi and plants. The EcM origins of *Hygrophorus*, *Hebeloma*, Paxillineae, and *Entoloma* were estimated to be in the Early Paleogene, somewhat similar to the divergence times of the major EcM plant lineages in Myrtaceae (e.g. *Eucalyptus*; Tedersoo & Brundrett, 2017). Although caution should be exercised due to errors produced in estimating divergence times and introduced by missing taxa, these findings suggest the coevolution of EcM Agaricomycetes and EcM plants.

The timing of evolutionary diversification suggested in this study has important implications for understanding the mechanism of the evolutionary diversification in Agaricomycetes. Neither of the rapid diversification in the Jurassic period (Varga *et al.*, 2019) nor the rapid diversification induced by the evolution of agaricoid fruitbodies (Varga *et al.*, 2019; Sánchez-García *et al.*, 2020) was not strongly supported in this study. Instead, increased diversification rates were suggested to occur intensively at the stems of EcM fungal clades that diverged in the Late Cretaceous (Figs 2–7). This contradicts the assumption that ecological opportunities for evolutionary diversification could be created simply by the evolution of EcM symbiosis. Under this assumption, the most ancient EcM fungi lineages (i.e. the EcM Cantharellales) could preempt the vacant niche space and obtain the greatest ecological opportunities according to the theory of the evolutionary priority effect (Fukami, 2015; De Meester *et al.*, 2016). Notably, in this study, the HiSSE model was more appropriate than the BiSSE model (Table 2), suggesting that the evolution of EcM symbiosis facilitated the rapid diversification under restricted conditions. For instance, the evolution of mutualistic relationship between EcM angiosperm and EcM fungal lineages that diverged in the Late Cretaceous (e.g. recognition of angiosperm hosts and repression of plant defenses) might have allowed for expanding the geographical ranges, resulting in the explosive diversification (that is, the mechanism of coevolutionary diversification; Yoder & Nuismer, 2010; Althoff *et al.*, 2014; Hembry *et al.*, 2014; Hembry & Weber, 2020). Although definitive evidence is elusive, these findings support the hypothesis that the evolution of symbiotic relationships between EcM fungi and angiosperms in the Late Cretaceous might facilitate the explosive diversification of Agaricomycetes.

Table 2 Model comparison of character-dependent diversification rate models in Agaricomycetes based on the Akaike information criteria (AIC).

	Original tree		TACT tree		Varga TACT tree	
Model	AIC	ΔAIC	AIC	ΔAIC	AIC	ΔAIC
CID						
CID2	4163.7	76.1	144 017.6	935.1	285 559.4	2341.1
CID4	4142.6	55.1	143 197.2	114.7	283 453.0	234.7
ECM						
BiSSE (ARD)	4134.0	46.4	145 005.6	1923.1	288 315.8	5097.5
BiSSE (ER)	4136.6	49.0	145 024.7	1942.2	288 337.7	5119.4
BiSSE (UD)	4132.0	44.4	145 015.0	1932.5	288 344.2	5125.9
HiSSE (ARD)	4093.4	5.9	143 084.8	2.3	283 218.3	0
HiSSE (ER)	4090.5	3.0	143 695.1	612.6	283 389.9	171.6
HiSSE (UD)	4087.6	0	143 082.5	0	283 341.4	123.1
Agaricoid s.l.						
BiSSE (ARD)	4175.8	88.3	145 247.8	2165.3	293 123.6	9905.3
BiSSE (ER)	4176.6	89.0	145 246.0	2163.5	293 324.5	10 106.2
HiSSE (ARD)	4130.9	43.3	143 389.2	306.7	287 230.3	4012.0
HiSSE (ER)	4127.7	40.1	143 446.2	363.7	287 422.3	4204.0
Agaricoid s.s.						
BiSSE (ARD)	4149.4	61.9	145 333.5	2251.0	293 429.4	10 211.1
BiSSE (ER)	4147.7	60.1	145 332.4	2249.9	293 608.0	10 389.7
HiSSE (ARD)	4103.4	15.8	143 477.6	395.1	287 641.3	4423.0
HiSSE (ER)	4104.5	16.9	143 787.6	705.1	287 662.8	10 389.7

AIC score and AIC difference between a model with lowest AIC score (most appropriate model) and focal model (ΔAIC) are shown. Here, two binary states, ectomycorrhizal (EcM) or not vs agaricoid fruitbody or not, were considered. For agaricoid, two definitions, agaricoid s.l. (pileate-stipitate and pileate-sessile) and agaricoid s.s. (pileate-stipitate only) were prepared. The diversification rate models compared here were a character-independent diversification model with two (CID-2) or four (CID-4) hidden states, the binary state speciation–extinction (BiSSE) model and the Hidden State Speciation and Extinction (HiSSE) model with four hidden states. As character-transition models, all rate different (ARD), equal rate (ER), and unidirectional evolution toward EcM (UD) models were included. The analysis was carried out on the Phylogenetic tree obtained in this study (original tree), the TACT tree of this study (TACT tree), and the TACT tree of Varga *et al*. (2019; Varga TACT tree), separately.

The acquisition of EcM symbiosis in the Late Cretaceous cannot explain all the shifts in diversification rates in Agaricomycetes. For instance, a less distinct increase in diversification rates was shown in several clades, including the EcM fungal clade (*Amanita*) and non-EcM fungal clades (Polyporaceae, *Entoloma*, and Agaricaceae; Figs 3, 4, S8, S9). Decreased diversification rates were indicated in the fungal taxa that do not produce airborne spores (Phallales and Nidulaceae), the EcM fungal clade with ancient EcM origins (Cantharellales), and some large clades consisting of wood-decaying fungi (Auriculariales, Schizoporaceae, and Gloeophyllaceae; Fig. 5; Table S6). The decreased diversification rates in taxa without airborne spores might be explained by decreased spore dispersibility and decelerated geographical expansion, partially agreeable with the fruitbody-type-induced diversification hypothesis (Varga *et al*., 2019, 2022; Sánchez-García *et al*., 2020). Moreover, the decreased diversification rates in other taxa, such as Cantharellales and Auriculariales, might have been caused by the lack of enclosed development of fruitbodies (Varga *et al*., 2022). The other patterns are perhaps due to the development of key innovations and unique traits that could have led to explosive diversification (Simpson, 1953; Schluter, 2000; Stroud & Losos, 2016). For instance, adaptive evolution of genes encoding plant cell wall-degrading enzymes in some saprotrophs could have resulted in replacing niche spaces occupied by preexisting saprotrophs. Unfortunately, genomic studies have not provided evidence for this hypothesis (Kohler *et al*., 2015; Martin *et al*., 2016; Nagy *et al*., 2016). Further studies, both evolutionary and genomic, are required to identify the drivers of these evolutionary dynamics.

Notably, the diversification rates of several non-EcM agaricoid fungal taxa were estimated to be much higher in other studies than in this study (Varga *et al*., 2019; Sánchez-García *et al*., 2020). These discrepancies are explained by differences in addressing incomplete taxon sampling (i.e. calculated based on OTU richness vs number of described species). Indeed, when the sampling fractions were calculated based on the number of described species (Fig. S8), high diversification rates were observed in non-EcM agaricoid fungal taxa, such as Mycenaceae, *Gymnopus* (Omphalotaceae), *Marasmius* (Marasmiaceae), and *Agaricus* (Agaricaceae), for which improved taxonomy is needed (Hawksworth, 2001). Similarly, the increased diversification rates of these fungal taxa became somewhat obscure in the Varga TACT tree (Fig. 4b). Moreover, using BiSSE or similar methods might result in overlooking complicated evolutionary scenarios in favor of unrealistic oversimplified ones (Rabosky & Goldberg, 2015; Beaulieu & O'Meara, 2016). Some taxonomic misidentifications (misclassification of trophic states) and/or phylogenetic uncertainties in megaphylogenies may disrupt the unidirectional evolution of EcM states, resulting in the spurious diversification rates of EcM fungi. These methodological issues might have obscured the rapid diversification of EcM fungi in the Late Cretaceous.

The limitations in the estimating net diversification rates must be discussed. First, an extremely low sampling fraction in the phylogenetic tree can cause estimation bias, particularly in the BAMM (Moore *et al*., 2016; Meyer & Wiens, 2018; Chang *et al*., 2020). However, in this study, major shifts in diversification rates were observed with the megaphylogeny of Varga *et al*. (2019). Similar results were obtained with five types of approaches, including MEDUSA and method-of-moment estimator, which are known to be relatively robust to low sampling fractions (Moore *et al*., 2016; Meyer & Wiens, 2018; Chang *et al*., 2020). They suggest that the biases caused by incomplete taxon sampling are limited here. In addition, recent work indicates that deep temporal trends in diversification rate shifts

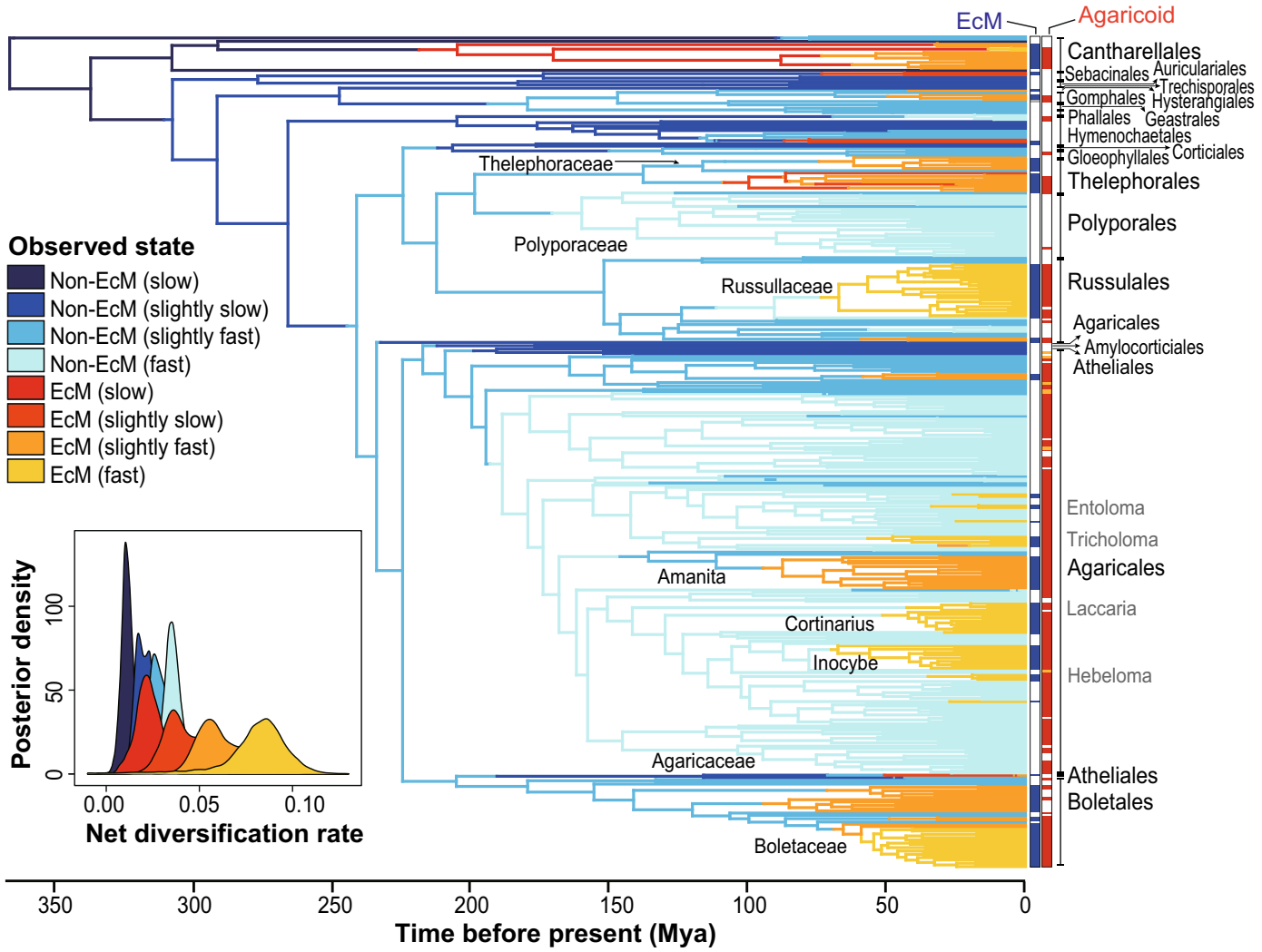

Fig. 7 Historical character transition of ectomycorrhizal (EcM) symbiosis and dynamics of net diversification rates (i.e. speciation rate minus extinction rate) in Agaricomycetes estimated by the Hidden State Speciation and Extinction (HiSSE) model assuming unidirectional evolution of EcM state. Branch colors in the phylogeny represent transition of characters along the edges of the tree and net diversification rates. A binary state (EcM vs non-EcM) besides four hidden characters are assumed, and thus, eight characters are identified in total. The density plot represents posterior distribution of diversification rates for respective characters.

cannot be accurately estimated with the phylogeny of extant species (Louca & Pennell, 2020). In this study, however, this concern is addressed by estimating tip rates. Another potential issue is that the method-of-moments estimator assumed extremely high extinction rates in this study because the estimated diversification rates had a strong negative correlation with clade ages in low ε values (Fig. S1), consistent with patterns of other organisms (Rabosky & Benson, 2021). The strong correlation between clade ages and diversification rates with low ε values is attributable to the short but intensive burst of speciation and mass extinction that occurred in Agaricomycetes, which could have led to underestimating diversification rates in older clades with this approach (Rabosky & Benson, 2021). Although this study aimed to mitigate the risk of misleading findings, more fossil evidence and further development of techniques are needed to elucidate the complete picture of evolutionary diversification in Agaricomycetes.

Conclusions

Molecular phylogenies inferred from fragments of 89 single-copy genes suggested that EcM symbiosis evolved multiple times independently and unidirectionally in Agaricomycetes, with origin times ranging from the Early Triassic to the Early Paleogene. However, a substantial increase in net diversification rates appeared to occur intensively at the stem of EcM fungal clades that diverged in the Late Cretaceous, suggesting that the greatest opportunities for niche expansion and subsequent explosive diversification were available only to these EcM fungi. The timing of rapid diversification inferred in Agaricomycetes corresponds well to that of the major EcM angiosperm lineages. This finding corroborates the scenario that coevolutionary interactions could have occurred between EcM fungi and EcM angiosperms that simultaneously diverged in the Late Cretaceous, resulting in the increased diversification rates of EcM fungi. By contrast, the

results of this study only partially support the hypothesis that the evolution of fruitbody forms could have caused the rapid diversification in Agaricomycetes. Although evolutionary and genomic studies that use more fossil evidence and developed techniques are needed, the coevolutionary diversification scenario of EcM fungi and EcM angiosperms suggested in this study has significant implications for understanding the origin of EcM fungi and EcM plant biodiversity.

Acknowledgements

I am grateful to Dr Kentaro Hosaka (National Museum of Nature and Science, Tokyo) and Dr Naoki Endo (Tottori University) for providing fungal DNA samples. I also wish to thank Dr Yoriko Sugiyama (Kyoto University), Mr. Otomi Satomi (Kyoto University), and members of the Kansai Mycological Club for collecting fungal specimens. I thank Dr Hiroki Yamanaka (Center for Biodiversity Science, Ryukoku University) for supporting the laboratory work, especially the high-throughput sequencing using the Illumina MiSeq. Computation time was provided by the SuperComputer System, Institute for Chemical Research, Kyoto University. This work was financially supported by a research grant from the Institute for Fermentation, Osaka (G-2019-1-029), a Grant-in-Aid for Scientific Research (20K06796), and JST/JICA, SATREPS (JPMJSA1902).

Competing interests

None declared.

Author contributions

HS planned and designed the research, performed the experiments, analyzed the data, interpreted the results, and wrote the manuscript.

ORCID

Hirotoshi Sato https://orcid.org/0000-0003-4489-6569

Data availability

Raw sequencing reads obtained from the Illumina MiSeq are deposited into the DDBJ Sequence Read Archive (Accession: DRA014552). Input and output files of molecular phylogenetic inference are available in the Dryad repository (https://datadryad.org/stash/share/S2aFpxT_WnUXo_I84TUiC1__KL-o1isHJPyWmSwvfIw). Supplemental figures and tables are available as a Supporting Information file.

References

Alfaro ME, Santini F, Brock C, Alamillo H, Dornburg A, Rabosky DL, Carnevale G, Harmon LJ. 2009. Nine exceptional radiations plus high turnover explain species diversity in jawed vertebrates. *Proceedings of the National Academy of Sciences, USA* **106**: 13410–13414.

Althoff DM, Segraves KA, Johnson MTJ. 2014. Testing for coevolutionary diversification: linking pattern with process. *Trends in Ecology & Evolution* **29**: 82–89.

Beaulieu JM, O'Meara BC. 2016. Detecting hidden diversification shifts in models of trait-dependent speciation and extinction. *Systematic Biology* **65**: 583–601.

Bengtsson-Palme J, Ryberg M, Hartmann M, Branco S, Wang Z, Godhe A, De Wit P, Sánchez-García M, Ebersberger I, de Sousa F. 2013. Improved software detection and extraction of ITS1 and ITS2 from ribosomal ITS sequences of fungi and other eukaryotes for analysis of environmental sequencing data. *Methods in Ecology and Evolution* **4**: 914–919.

Bollback JP. 2006. SIMMAP: stochastic character mapping of discrete traits on phylogenies. *BMC Bioinformatics* **7**: 1.

Bouckaert R, Heled J, Kühnert D, Vaughan T, Wu C-H, Xie D, Suchard MA, Rambaut A, Drummond AJ. 2014. BEAST 2: a software platform for Bayesian evolutionary analysis. *PLoS Computational Biology* **10**: e1003537.

Campbell V, Legendre P, Lapointe F-J. 2011. The performance of the Congruence Among Distance Matrices (CADM) test in phylogenetic analysis. *BMC Evolutionary Biology* **11**: 64.

Cao B, Haelewaters D, Schoutteten N, Begerow D, Boekhout T, Giachini AJ, Gorjón SP, Gunde-Cimerman N, Hyde KD, Kemler M. 2021. Delimiting species in Basidiomycota: a review. *Fungal Diversity* **109**: 1–57.

Chang J, Rabosky DL, Alfaro ME. 2020. Estimating diversification rates on incompletely sampled phylogenies: theoretical concerns and practical solutions. *Systematic Biology* **69**: 602–611.

De Meester L, Vanoverbeke J, Kilsdonk LJ, Urban MC. 2016. Evolving perspectives on monopolization and priority effects. *Trends in Ecology & Evolution* **31**: 136–146.

Ehrlich PR, Raven PH. 1964. Butterflies and plants: a study in coevolution. *Evolution* **18**: 586–608.

Fukami T. 2015. Historical contingency in community assembly: integrating niches, species pools, and priority effects. *Annual Review of Ecology, Evolution, and Systematics* **46**: 1–23.

Hamady M, Walker JJ, Harris JK, Gold NJ, Knight R. 2008. Error-correcting barcoded primers for pyrosequencing hundreds of samples in multiplex. *Nature Methods* **5**: 235–237.

Hawksworth DL. 2001. Mushrooms: the extent of the unexplored potential. *International Journal of Medicinal Mushrooms* **3**: 5.

Hembry DH, Weber MG. 2020. Ecological interactions and macroevolution: a new field with old roots. *Annual Review of Ecology, Evolution, and Systematics* **51**: 215–243.

Hembry DH, Yoder JB, Goodman KR. 2014. Coevolution and the diversification of life. *American Naturalist* **184**: 425–438.

Höhna S, Landis MJ, Heath TA, Boussau B, Lartillot N, Moore BR, Huelsenbeck JP, Ronquist F. 2016. REVBAYES: Bayesian phylogenetic inference using graphical models and an interactive model-specification language. *Systematic Biology* **65**: 726–736.

Hsieh T, Ma K, Chao A. 2016. iNEXT: an R package for rarefaction and extrapolation of species diversity (Hill numbers). *Methods in Ecology and Evolution* **7**: 1451–1456.

Janz N. 2011. Ehrlich and Raven revisited: mechanisms underlying codiversification of plants and enemies. *Annual Review of Ecology, Evolution, and Systematics* **42**: 71–89.

Jetz W, Thomas GH, Joy JB, Hartmann K, Mooers AO. 2012. The global diversity of birds in space and time. *Nature* **491**: 444–448.

Kadowaki K, Yamamoto S, Sato H, Tanabe AS, Hidaka A, Toju H. 2018. Mycorrhizal fungi mediate the direction and strength of plant–soil feedbacks differently between arbuscular mycorrhizal and ectomycorrhizal communities. *Communications Biology* **1**: 196.

Kohler A, Kuo A, Nagy LG, Morin E, Barry KW, Buscot F, Canbäck B, Choi C, Cichocki N, Clum A. 2015. Convergent losses of decay mechanisms and rapid turnover of symbiosis genes in mycorrhizal mutualists. *Nature Genetics* **47**: 410–415.

Larson-Johnson K. 2016. Phylogenetic investigation of the complex evolutionary history of dispersal mode and diversification rates across living and fossil Fagales. *New Phytologist* **209**: 418–435.

Liang M, Johnson D, Burslem DF, Yu S, Fang M, Taylor JD, Taylor AF, Helgason T, Liu X. 2020. Soil fungal networks maintain local dominance of ectomycorrhizal trees. *Nature Communications* **11**: 1–7.

van der Linde S, Suz LM, Orme CDL, Cox F, Andreae H, Asi E, Atkinson B, Benham S, Carroll C, Cools N. 2018. Environment and host as large-scale controls of ectomycorrhizal fungi. *Nature* **558**: 243–248.

Losos JB. 2010. Adaptive radiation, ecological opportunity, and evolutionary determinism. *American Naturalist* **175**: 623–639.

Louca S, Pennell MW. 2020. Extant timetrees are consistent with a myriad of diversification histories. *Nature* **580**: 502–505.

Lutzoni F, Nowak MD, Alfaro ME, Reeb V, Miadlikowska J, Krug M, Arnold AE, Lewis LA, Swofford DL, Hibbett D. 2018. Contemporaneous radiations of fungi and plants linked to symbiosis. *Nature Communications* **9**: 5451.

Magallon S, Sanderson MJ. 2001. Absolute diversification rates in angiosperm clades. *Evolution* **55**: 1762–1780.

Martin F, Kohler A, Murat C, Veneault-Fourrey C, Hibbett DS. 2016. Unearthing the roots of ectomycorrhizal symbioses. *Nature Reviews Microbiology* **14**: 760–773.

May MR, Moore BR. 2016. How well can we detect lineage-specific diversification-rate shifts? A simulation study of sequential AIC methods. *Systematic Biology* **65**: 1076–1084.

Meyer AL, Wiens JJ. 2018. Estimating diversification rates for higher taxa: BAMM can give problematic estimates of rates and rate shifts. *Evolution* **72**: 39–53.

Moore BR, Höhna S, May MR, Rannala B, Huelsenbeck JP. 2016. Critically evaluating the theory and performance of Bayesian analysis of macroevolutionary mixtures. *Proceedings of the National Academy of Sciences, USA* **113**: 9569–9574.

Nagy LG, Riley R, Tritt A, Adam C, Daum C, Floudas D, Sun H, Yadav JS, Pangilinan J, Larsson K-H. 2016. Comparative genomics of early-diverging mushroom-forming fungi provides insights into the origins of lignocellulose decay capabilities. *Molecular Biology and Evolution* **33**: 959–970.

O'Meara BC, Beaulieu JM. 2016. Past, future, and present of state-dependent models of diversification. *American Journal of Botany* **103**: 792–795.

Paradis E, Claude J, Strimmer K. 2004. APE: analyses of phylogenetics and evolution in R language. *Bioinformatics* **20**: 289–290.

Pennell MW, Eastman JM, Slater GJ, Brown JW, Uyeda JC, FitzJohn RG, Alfaro ME, Harmon LJ. 2014. GEIGER v.2.0: an expanded suite of methods for fitting macroevolutionary models to phylogenetic trees. *Bioinformatics* **30**: 2216–2218.

Põlme S, Abarenkov K, Nilsson RH, Lindahl BD, Clemmensen KE, Kauserud H, Nguyen N, Kjøller R, Bates ST, Baldrian P. 2020. FUNGALTRAITS: a user-friendly traits database of fungi and fungus-like stramenopiles. *Fungal Diversity* **105**: 1–16.

Põlme S, Bahram M, Yamanaka T, Nara K, Dai YC, Grebenc T, Kraigher H, Toivonen M, Wang P-H, Matsuda Y *et al.* 2013. Biogeography of ectomycorrhizal fungi associated with alders (*Alnus* spp.) in relation to biotic and abiotic variables at the global scale. *New Phytologist* **198**: 1239–1249.

R Development Core Team. 2020. *R (v.4.0.)[Computer software]*. Vienna, Austria: R Foundation for Statistical Computing. [WWW document] URL http://www.R-project.org [accessed 6 July 2022].

Rabosky DL, Benson RB. 2021. Ecological and biogeographic drivers of biodiversity cannot be resolved using clade age-richness data. *Nature Communications* **12**: 1–10.

Rabosky DL, Goldberg EE. 2015. Model inadequacy and mistaken inferences of trait-dependent speciation. *Systematic Biology* **64**: 340–355.

Rabosky DL, Grundler M, Anderson C, Shi JJ, Brown JW, Huang H, Larson JG. 2014. BAMMTOOLS: an R package for the analysis of evolutionary dynamics on phylogenetic trees. *Methods in Ecology and Evolution* **5**: 701–707.

Rabosky DL, Mitchell JS, Chang J. 2017. Is BAMM flawed? Theoretical and practical concerns in the analysis of multi-rate diversification models. *Systematic Biology* **66**: 477–498.

Revell LJ. 2012. PHYTOOLS: an R package for phylogenetic comparative biology (and other things). *Methods in Ecology and Evolution* **3**: 217–223.

Rinaldi AC, Comandini O, Kuyper TW. 2008. Ectomycorrhizal fungal diversity: separating the wheat from the chaff. *Fungal Diversity* **33**: 1–45.

Sánchez-García M, Matheny PB. 2017. Is the switch to an ectomycorrhizal state an evolutionary key innovation in mushroom-forming fungi? A case study in the Tricholomatineae (Agaricales). *Evolution* **71**: 51–65.

Sánchez-García M, Ryberg M, Khan FK, Varga T, Nagy LG, Hibbett DS. 2020. Fruiting body form, not nutritional mode, is the major driver of diversification in mushroom-forming fungi. *Proceedings of the National Academy of Sciences, USA* **117**: 32528–32534.

Sato H, Murakami N. 2008. Reproductive isolation among cryptic species in the ectomycorrhizal genus *Strobilomyces*: population-level CAPS marker-based genetic analysis. *Molecular Phylogenetics and Evolution* **48**: 326–334.

Sato H, Ohta R, Murakami N. 2020. Molecular prospecting for cryptic species of the *Hypholoma fasciculare* complex: toward the effective and practical delimitation of cryptic macrofungal species. *Scientific Reports* **10**: 13224.

Sato H, Tanabe AS, Toju H. 2017. Host shifts enhance diversification of ectomycorrhizal fungi: diversification rate analysis of the ectomycorrhizal fungal genera *Strobilomyces* and *Afroboletus* with an 80-gene phylogeny. *New Phytologist* **214**: 443–454.

Sato H, Toju H. 2019. Timing of evolutionary innovation: scenarios of evolutionary diversification in a species-rich fungal clade, Boletales. *New Phytologist* **222**: 1924–1935.

Sato H, Tsujino R, Kurita K, Yokoyama K, Agata K. 2012. Modelling the global distribution of fungal species: new insights into microbial cosmopolitanism. *Molecular Ecology* **21**: 5599–5612.

Schluter D. 2000. *The ecology of adaptive radiation*. New York, NY, USA: Oxford University Press.

Simpson GG. 1953. *The major features of evolution*. New York, NY, USA: Columbia University Press.

Smith SE, Read DJ. 2008. *Mycorrhizal Symbiosis, 3rd edn*. London, UK: Academic Press.

Stamatakis A. 2006. RAxML-VI-HPC: maximum likelihood-based phylogenetic analyses with thousands of taxa and mixed models. *Bioinformatics* **22**: 2688–2690.

Stroud JT, Losos JB. 2016. Ecological opportunity and adaptive radiation. *Annual Review of Ecology, Evolution, and Systematics* **47**: 507–532.

Tanabe AS. 2011. KAKUSAN4 and AMINOSAN: two programs for comparing nonpartitioned, proportional and separate models for combined molecular phylogenetic analyses of multilocus sequence data. *Molecular Ecology Resources* **11**: 914–921.

Tanabe AS, Toju H. 2013. Two new computational methods for universal DNA barcoding: a benchmark using barcode sequences of bacteria, archaea, animals, fungi, and land plants. *PLoS ONE* **8**: e76910.

Tedersoo L, Bahram M, Põlme S, Kõljalg U, Yorou NS, Wijesundera R, Ruiz LV, Vasco-Palacios AM, Thu PQ, Suija A. 2014. Global diversity and geography of soil fungi. *Science* **346**: 1256688.

Tedersoo L, Brundrett MC. 2017. Evolution of ectomycorrhizal symbiosis in plants. In: *Biogeography of mycorrhizal symbiosis*. Cham, Switzerland: Springer, 407–467.

Tedersoo L, May TW, Smith ME. 2010. Ectomycorrhizal lifestyle in fungi: global diversity, distribution, and evolution of phylogenetic lineages. *Mycorrhiza* **20**: 217–263.

Tedersoo L, Smith ME. 2013. Lineages of ectomycorrhizal fungi revisited: foraging strategies and novel lineages revealed by sequences from belowground. *Fungal Biology Reviews* **27**: 83–99.

Thompson JN. 1994. *The coevolutionary process*. Chicago, IL, USA: University of Chicago Press.

Varga T, Földi C, Bense V, Nagy LG. 2022. Radiation of mushroom-forming fungi correlates with novel modes of protecting sexual fruiting bodies. *Fungal Biology* **126**: 556–565.

Varga T, Krizsán K, Földi C, Dima B, Sánchez-García M, Sánchez-Ramírez S, Szöllősi GJ, Szarkándi JG, Papp V, Albert L. 2019. Megaphylogeny resolves global patterns of mushroom evolution. *Nature Ecology & Evolution* **3**: 668–678.

Vasconcelos T, O'Meara BC, Beaulieu JM. 2022. A flexible method for estimating tip diversification rates across a range of speciation and extinction scenarios. *Evolution* **76**: 1420–1433.

Yoder JB, Clancey E, Des Roches S, Eastman JM, Gentry L, Godsoe W, Hagey TJ, Jochimsen D, Oswald BP, Robertson J. 2010. Ecological opportunity and

the origin of adaptive radiations. *Journal of Evolutionary Biology* **23**: 1581–1596.

Yoder JB, Nuismer SL. 2010. When does coevolution promote diversification? *American Naturalist* **176**: 802–817.

Zanne AE, Tank DC, Cornwell WK, Eastman JM, Smith SA, FitzJohn RG, McGlinn DJ, O'Meara BC, Moles AT, Reich PB. 2014. Three keys to the radiation of angiosperms into freezing environments. *Nature* **506**: 89–92.

Supporting Information

Additional Supporting Information may be found online in the Supporting Information section at the end of the article.

Fig. S1 Correlation between clade age and net diversification rate in Agaricomycetes estimated by the method-of-moment estimator.

Fig. S2 Maximum likelihood tree of Agaricomycetes inferred from fragments of 89 single-copy genes.

Fig. S3 Bayesian phylogenetic tree of Agaricomycetes inferred from fragments of 89 single-copy genes.

Fig. S4 Proportion of primary lifestyle and fruitbody form in orders in Agaricomycetes.

Fig. S5 Relationship of net diversification rates (i.e. speciation rate minus extinction rate) of fungal taxa belonging to Agaricomycetes estimated by the Bayesian Analysis of Macroevolutionary Mixtures using three different phylogenetic trees.

Fig. S6 Plots of net diversification rates through time in Agaricomycetes and Agaricomycetidae inferred using the Bayesian Analysis of Macroevolutionary Mixtures, in which taxon-specific sampling fraction is calculated based on richness of operational taxonomic units in the UNITE database.

Fig. S7 Plots of net diversification rates through time in Agaricomycetes and Agaricomycetidae inferred using the Bayesian Analysis of Macroevolutionary Mixtures, in which taxon-specific sampling fraction is calculated based on total number of described species in the Species Fungorum.

Fig. S8 Dynamics of net diversification rates (i.e. speciation rate minus extinction rate) in Agaricomycetes estimated using Bayesian Analysis of Macroevolutionary Mixtures and the modeling evolutionary diversification using stepwise AIC (MEDUSA), in which taxon-specific sampling fraction is calculated based on richness of operational taxonomic units in the UNITE database.

Fig. S9 Dynamics of net diversification rates (i.e. speciation rate minus extinction rate) in Agaricomycetes estimated using Bayesian Analysis of Macroevolutionary Mixtures and the modeling evolutionary diversification using stepwise AIC (MEDUSA), in which taxon-specific sampling fraction is calculated based on total number of described species in the Species Fungorum.

Methods S1 Supplementary methods for estimation of historical patterns of states and estimation of net diversification rates.

Table S1 Sample lists used in this study.

Table S2 List of PCR primers used in this study.

Table S3 Fossil records used for calibration points of divergence time estimation.

Table S4 Richness of operational taxonomic units estimated by the iNEXT R package.

Table S5 Taxon-specific sampling fraction calculated based on the richness of operational taxonomic units (OTUs) estimated by the iNEXT R package, OTU richness observed in the UNITE database, and the total number of described species in the Species Fungorum.

Table S6 Clade age mean, estimated richness of operational taxonomic units, trophic state (ectomycorrhizal or not), fruitbody type (agaricoid or not), and net diversification rates of focal clades estimated by the method-of-moment estimator and Bayesian Analyses of Macroevolutionary Mixtures.

Please note: Wiley is not responsible for the content or functionality of any Supporting Information supplied by the authors. Any queries (other than missing material) should be directed to the *New Phytologist* Central Office.